

UC Davis

UC Davis Previously Published Works

Title

Influence of synthesis temperature on the defect structure of boron carbide:
Experimental and modeling studies

Permalink

<https://escholarship.org/uc/item/4895t7nq>

Journal

Journal of the American Ceramic Society, 88(6)

ISSN

0002-7820

Authors

Anselmi-Tamburini, U
Munir, Zuhair A
Kodera, Y
[et al.](#)

Publication Date

2005-06-01

Peer reviewed

Influence of Synthesis Temperature on the Defect Structure of Boron Carbide: Experimental and Modeling Studies

Umberto Anselmi-Tamburini[†] and Zuhair A. Munir[‡]

Department of Chemical Engineering and Materials Science, University of California, Davis, California 95616

Yasuhiro Kodera, Takahito Imai, and Manshi Ohyanagi

Department of Materials Chemistry and the High-Tech Research Center, Ryukoku University, Seta, Ohtsu, Japan

Boron carbide (B_4C) was synthesized from the elements at temperatures ranging from 1300° to 2100°C using the spark plasma synthesis method. Significant densification commenced at about 1500°C and was accompanied by a corresponding decrease in the defect structure of this carbide. Changes in the X-ray diffraction patterns were in agreement with predictions of simulation studies based on the presence of twins. Transmission electron microscopy observations were consistent with the experimental observations and the modeling predictions.

I. Introduction

BORON-RICH carbon compounds continue to attract significant attention because of theoretical and practical considerations. In both cases, the focus has been on the unique structure of these compounds. The structure is based on boron-rich icosahedra, which can be bonded by carbon and boron atoms (as in the case of boron carbide (B_4C)) or other atoms (as in the case of the recently investigated boride, $AlMgB_{14}$). B_4C is a very hard material (being third hardest after diamond and cubic BN) with a high melting point (above 2400°C), and as such has found application as an abrasive material. It is also a wide gap p-type semiconductor with an anomalously large Seebeck coefficient and thus has potential application in high-temperature thermoelectric devices.² B_4C is also used in control rods for nuclear power generation.³

Despite the large number of existing reports on this material, several issues related to the structure and characteristics of this carbide remain unresolved. In part, this is due to the complexity of its structure and its relatively wide phase stability region. While nominally assigned the formula B_4C , the compound has a wide range of homogeneity, the extent of which is subject to controversy and is one of the unresolved issues. It is generally assumed that B_4C stoichiometry ranges from B_4C to $B_{10.5}C_3$, corresponding to a range of about 20–9 at.% C, respectively.³ Because of this, point defects and crystallographic disorder are expected to be present and to play an important role in defining its properties, such as its electrical and thermal behavior.⁴ While the nature of these defects and their effect on macroscopic properties have been recognized for some time, their dependence on the synthesis conditions of the carbide phase and their characterization by X-ray diffraction (XRD) methods have received much less attention.

The presence of plane defects in such materials as B_4C and SiC has been well recognized. In the case of B_4C , it was shown through high-resolution transmission electron microscopy (HRTEM) that these defects are twins,⁵ while those in SiC have been identified as stacking faults.⁶ Two aspects related to the presence of these defects are of interest: their effect on the XRD patterns and their role in the densification through mass transport. An important implication in the former relates to the use of XRD patterns to calculate crystallite size, and in the latter to the acceleration of sintering and the avoidance of exaggerated grain growth. An example of the effect of defects on XRD patterns comes from a recent study on the synthesis of B_4C by mechanical and field activation.⁷ Crystallite size analysis from XRD line broadening using the Halder–Wagner method gave values that were in sharp contrast to TEM observations. The calculated values from XRD analysis, 20–40 nm, are in contrast to TEM observation showing a size range from >100 nm to several micrometers. And an example of the effect of defects on sintering comes from a recent study on SiC.⁸ The observed rapid increase in density over a narrow range of sintering temperature was associated with a disorder–order transformation in which stacking fault density decreased dramatically.⁸

In this paper, we present experimental observations on the effect of synthesis temperature on the XRD pattern of B_4C and thus its defect concentration. The results are interpreted in light of simulation and TEM observations.

II. Experimental Procedures

B_4C was synthesized and processed using two approaches. In the first approach, synthesis of B_4C from elemental powders was accomplished by field activation using the spark plasma synthesis (SPS) method at different temperatures. In the second approach the samples were synthesized in the SPS at a fixed (low) temperature (1300°C) and then subsequently annealed in a high-vacuum furnace for 30 min at higher temperatures (1300–2100°C).

The SPS method is a relatively new technique that has shown considerable success in the synthesis and processing of a variety of high-density refractory materials, including bulk nanostructures.^{7,9–11} In this technique, heating of a sample contained in a graphite die is accomplished by passing a pulsed high DC current while applying a uniaxial pressure. The SPS system we utilized is a model 1050 (Sumitomo Heavy Industry, Tokyo, Japan). In a typical synthesis experiment, about 2.5 g of carbon (carbon black, Thermax Ultra-pure N990, Cancarb, Ltd., Medicine Hat, Alberta, Canada, ash content below 0.02%) and amorphous boron (Atlantic Equipment Engineering, Bergenfield, NJ, 95% purity, 0.1- μ m particle size) mixture with the desired B/C = 4 stoichiometry were first thoroughly mixed in a mortar for several minutes. The mixture was then placed in a graphite die having an inside diameter of 19 mm. The die was then placed in the SPS and a uniaxial pressure of 70 MPa was

R. L. Snyder—contributing editor

Manuscript No. 10784. Received January 8, 2004; approved February 3, 2005.

This work was supported by a grant from the Army Research Office (Z. A. M.) and by a grant based on the High-Tech Research Center Program (M. O.).

[†]Visiting Professor, Permanent address: Department of Physical Chemistry, University of Pavia, Pavia, Italy.

[‡]Author to whom correspondence should be addressed. e-mail: zamunir@ucdavis.edu

applied. The system was then evacuated to a pressure of about 10^{-2} Torr. In order to ensure a more reliable temperature control and measurement, a modified setup was used. A hole was drilled axially through the lower plunger of the die and a very thin ($127\ \mu\text{m}$) C-type thermocouple was inserted into it such that the thermocouple is in direct contact with the lower surface of the sample. Each reactant mixture was then heated to a chosen temperature in the range of 1200°C – 1900°C and held there for 10 min. The heating rate was $200^{\circ}\text{C}/\text{min}$. During the entire process, the sample temperature, average applied voltage and current, and sample linear dimension were recorded in real time. Following cooling, samples were characterized by X-ray powder diffraction (XRD) using a diffractometer SCINTAG XDS 2000 (SCINTAG Inc., Cupertino, CA) equipped with a Cu tube and Ni filter. The TEM observations were made with a JEOL JEM4000EX microscope (Jeol USA, Inc., Peabody, MA) operated at 400 kV. Powders from the samples were dispersed in ethanol and placed on a carbon mesh for observation.

In order to identify the changes that a high degree of faulting can produce in the XRD patterns of B_4C , we performed computer simulation using the program DIFFaX.¹² This program can simulate the diffraction pattern of any structure containing planar faults (such as twins and stacking faults) and provide an evaluation of the incoherent intensity distribution due to faults with a random distribution. Our simulations were based on previous TEM observations that suggested the presence of twins on the basal (001) plane of the rhombohedral cell.^{12,14} Although the existence of twins in B_4C has been well established, their possible influence on the XRD pattern has never been investigated. Since the program does not accept structures with a γ angle different from 90° , a new elementary cell that lies on the (001) plane of the original rhombohedral structure of B_4C ¹⁴ and containing 30 atoms has been used to describe the structure. In the simulation we define α as the stacking probability. It is the probability that a given layer will be followed by a layer with the wrong stacking sequence. The diffraction intensities are then calculated for a statistical ensemble of crystallites, each with a distinct stacking sequence, but weighted by the probability that such sequence will occur. The program also can take into account the effect of crystallite sizes. The directions **a** and **b** lying on the twin plane are treated considering a Scherrer-type peak broadening due to a finite layer width. Small crystallite sizes in the direction perpendicular to the twin plane can be specified indicating the number of layers that must be included in each crystallite.

III. Results

Figure 1 shows typical changes of the experimental parameters (sample temperature, applied electrical power, and sample linear dimension) observed during the SPS synthesis of a sample at 1700°C . As will be seen below, formation of the carbide takes place at a lower temperature (about 1200°C) and thus reference to the “synthesis temperature” implies the target temperature at which the sample is held for 10 min. Because of the direct contact between the controlling thermocouple and the reacting sample, the relatively low exothermic heat effect produced by the synthesis reaction of B_4C , $71.2\ \text{kJ}/\text{mol}$,¹⁵ could be detected as a small hump in the temperature profile at about 1200°C (corresponding to a time of about 250 s). Since the thermocouple is also used to control the power feedback of the SPS, the slight, short-lived increase in temperature resulting from the exothermic reaction is compensated for by a transient decrease in the power as seen in the figure. And since the formation of the product represents a decrease in the molar volume (by about 8% in this case), a change in the linear dimension (contraction) is also observed at the same time. A second, much larger change (shrinkage) is observed beginning at about 1600°C corresponding to a densification of the produced B_4C . The densities of the samples synthesized at various temperatures (with a 10-min holding time) are shown in Fig. 2. When synthesized at temperatures up to about 1500°C , the samples had relatively low den-

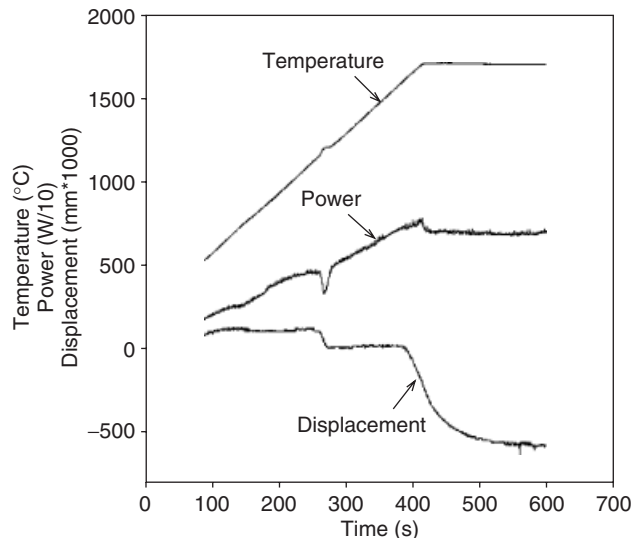


Fig. 1. Typical changes in the spark plasma synthesis parameters during the synthesis of boron carbide at 1700°C .

sities, but when synthesis was done at higher temperatures, a significant increase in density was achieved.

The XRD patterns of the samples synthesized at various temperatures are shown in Fig. 3. The patterns show significant changes as the temperature is increased from 1000° to 2100°C . The results show that B_4C forms at as low a temperature as 1000°C . However, at this temperature the conversion to carbide is only partial, as indicated by the presence of boron peaks at 2θ of about 20° (although nominally the boron was amorphous, pairs of which were crystalline). The formation of the carbide becomes complete when the synthesis temperature is 1200°C or higher. However, the pattern of the material synthesized at 1200°C has significant anomalies when compared with the theoretical pattern of B_4C , which is indicated by the lines on the bottom of the graph. Several small peaks are missing, other peaks appear to have merged, and two broad halos are observed at around 2θ values of 23° and 36° . When the synthesis temperature was increased between 1200° and 1400°C , the XRD patterns showed little change, but significant changes develop when the synthesis is made at higher temperatures. The features of the B_4C patterns obtained on samples produced at relatively low temperatures ($1400^{\circ} < T \leq 1700^{\circ}\text{C}$) can be better discerned by examining Fig. 4, which shows the 1600°C pattern with markers (arrows) identifying regions of major anomalies. The doublet centered at 23° appears well developed as well as the peaks at 2θ of about 20° and 32° . Further increase in temperature shows a

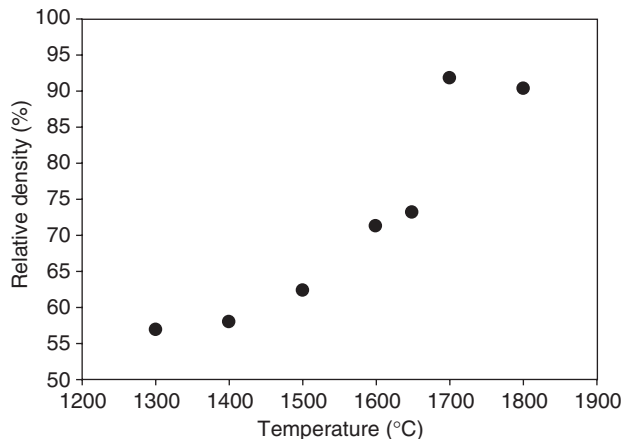


Fig. 2. Relative densities of samples synthesized at different temperatures (10-min hold time) under a pressure of 70 MPa.

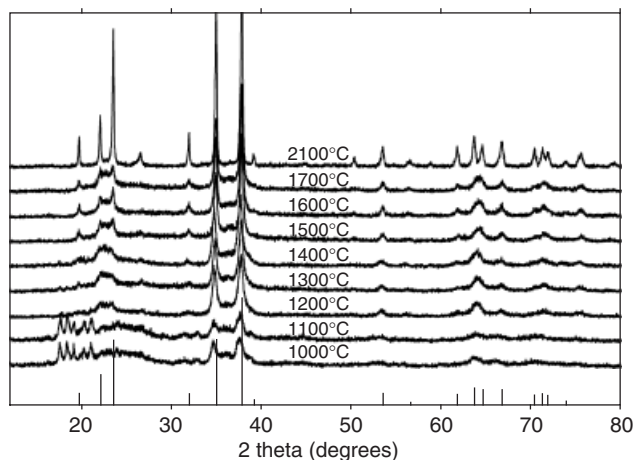


Fig. 3. X-ray diffraction patterns of boron carbide synthesized in the spark plasma synthesis at various temperatures.

progressive change in the pattern with the most significant change occurring between 1700° and 2100°C.

In addition to the changes described above, changes in peak width are also observed with the reaction temperature. This is illustrated in Fig. 5, in which the change of the full-width at half-maximum (FWHM) of the two main peaks (at about 35° and 38°) is plotted as a function of synthesis temperature for the (104) and (021) diffractions. A decrease of about a factor of four is seen in FWHM as the synthesis temperature is increased from 1000° to 2100°C.

As indicated in the Experimental Procedures section, the second series of experiments was made such that B_4C was first synthesized in the SPS at a relatively low temperature, 1300°C (where complete conversion takes place) and then annealed under high vacuum for 30 min at temperatures ranging from 1300° to 2100°C. This second set of experiments was designed to determine if the observed anomalies in the XRD results are the consequence of the SPS synthesis method. The XRD patterns obtained from the annealed samples are shown in Fig. 6. The patterns are consistent with those obtained when the synthesis was made directly in the SPS, as can be seen by comparing this figure with Fig. 5. The consistency between these two sets of results indicates that synthesis at higher temperatures is equivalent to the annealing of the product synthesized at lower temperatures. Similar results were obtained when samples with a stoichiometry corresponding to the limit of the stability of B_4C , i.e., B_9C , were synthesized and vacuum annealed in the same way, as seen in Fig. 7.

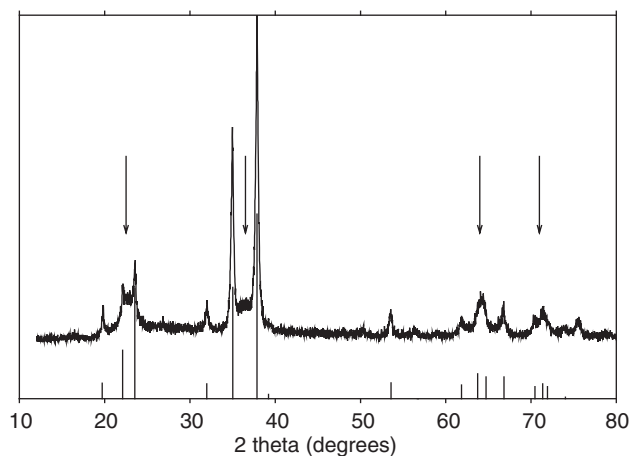


Fig. 4. X-ray diffraction pattern of a boron carbide sample synthesized at 1600°C in the spark plasma synthesis.

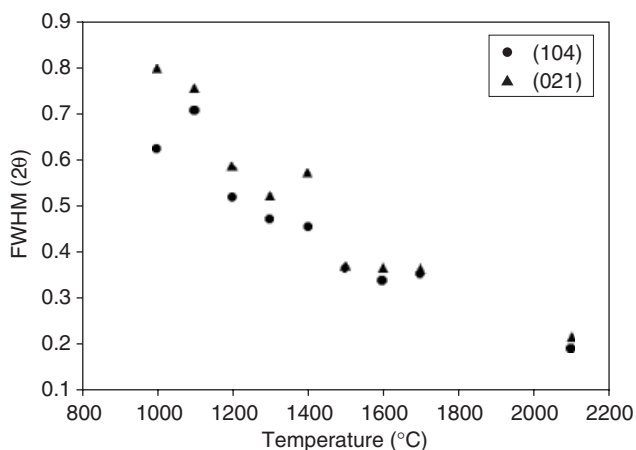


Fig. 5. Changes of the full-width at half-maximum of the two main peaks of boron carbide with synthesis temperature.

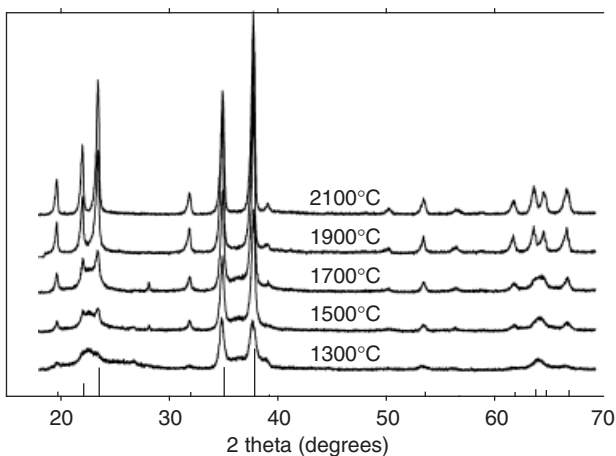


Fig. 6. X-ray diffraction patterns of boron carbide samples synthesized in the spark plasma synthesis at 1300°C and subsequently annealed in vacuum for 30 min at various temperatures.

IV. Discussion

The results show that the synthesis of B_4C from the elements using field activation can take place at as low a temperature as 1000°C and is complete at about 1200°C (with a 10-min hold time). The products obtained at low temperatures, however,

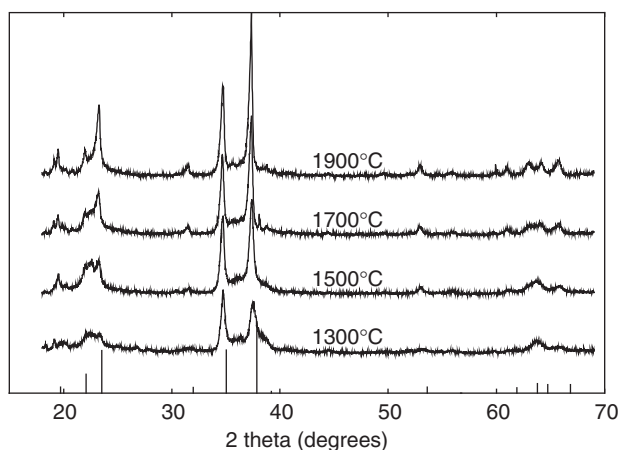


Fig. 7. X-ray diffraction patterns of samples with B_9C stoichiometry synthesized in the spark plasma synthesis at 1300°C and subsequently annealed in vacuum for 30 min at various temperatures.

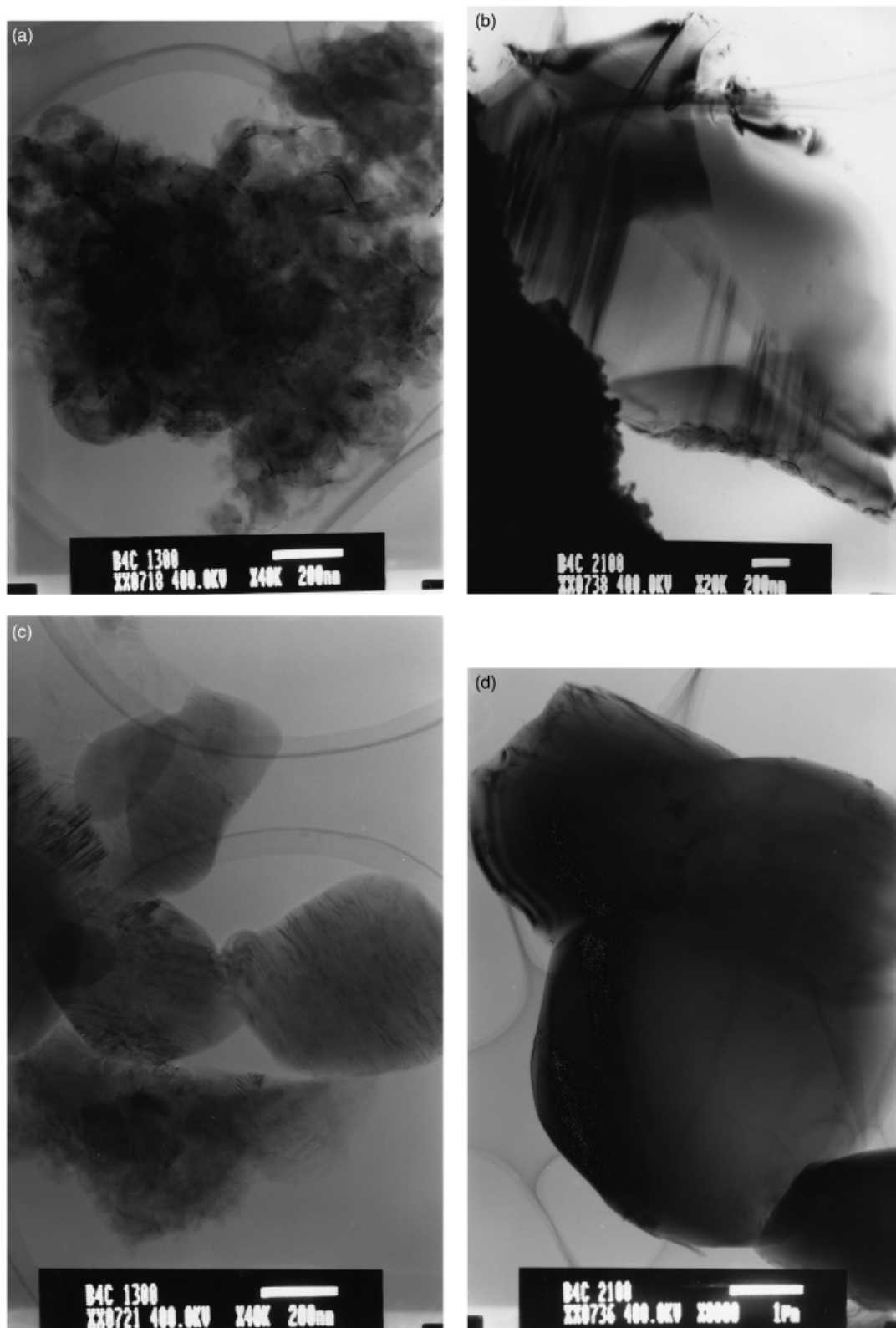


Fig. 8. Transmission electron microscopy micrographs of boron carbide samples: (a) synthesized at 1300°C showing small particle size. (b) Synthesized at 1300°C showing twins. (c) Synthesized at 2100°C. (d) Synthesized at 2100°C.

show considerable crystallographic disorder as evidenced by the X-ray powder patterns. No evidence of such a high degree of crystallographic disorder in B_4C has been reported before. Significant densification begins at a temperature of about 1600°C (Figs. 1 and 2). This temperature corresponds to the onset of a marked decrease in the crystallographic disorder, as indicated by the XRD patterns (Fig. 3). The simultaneous occurrence of densification and crystallographic order is a consequence of

rapid mass transport at this temperature to reduce internal energy. Although no densification studies were made on samples with the B_9C stoichiometry, the changes in the XRD patterns with annealing temperature are generally similar to those obtained for the B_4C stoichiometry, as can be seen by comparing Figs. 6 and 7.

The effect of phase transformation on reactivity, the Hedvall effect, has been investigated in earlier studies,¹⁶⁻¹⁹ and enhance-

ment of reactivity due to disorder has been reported.²⁰ In recent studies, it was shown that enhanced sintering is correlated with disorder–order transformation in β -SiC.^{8,21} A marked increase in sintering (with a change in relative density from about 60%–98%) occurred over the narrow temperature range of 1600°–1700°C. The XRD results showed a corresponding marked decrease in stacking fault density. The increase in densification of B_4C with temperature, observed in this study, was not as dramatic as that reported for SiC.⁸ This relates to the observed changes in the XRD patterns indicating corresponding changes in the defect nature of the two materials. In the case of SiC, little evidence remains for defects in samples sintered at higher temperatures, while in the case of B_4C , evidence for some disorder is still seen in the products synthesized at higher temperatures, as will be seen subsequently.

The dependence of the X-ray powder patterns of B_4C on synthesis temperature has not been treated in the literature, with the exception of an indication from the work of Prickett *et al.*²² on samples prepared through a different synthesis route. The nature of this disorder is probably complex and we will show that it cannot be characterized by a single defect. Two major features in the X-ray patterns of the samples synthesized at low temperatures are particularly evident: peak broadening and the appearance of large halos at positions corresponding to the two major doublets. The presence of broad peaks suggests the existence of nanometric grains. However, recent observations showed that this could not be used as conclusive evidence.⁷ While line-broadening analysis gave small grain sizes, TEM images showed the presence of nanometric grains as well as larger grains (up to a few micrometers). The larger grains showed the presence of high densities of twins, which contributed to the line broadening and hence to the erroneous calculation of small grain size.

TEM observations were made on samples synthesized at selected temperatures (low, 1300°C; intermediate, 1500°C; and high, 2100°C) in order to examine the changes in the presence of twins and to ascertain the grain size. Figures 8(a) and (b) show samples synthesized at 1300°C. Figure 8(a) shows the existence of small grains (<100 nm), while Fig. 8(b) shows the presence of high concentrations of twins in relatively large B_4C grains (about 1 μ m in size). The presence of twins in samples synthesized at 1500°C was also confirmed by TEM observations. When synthesis was made at the highest temperature, 2100°C, the sample contained twins, but at a much lower concentration, as can be seen in Figs. 8(c) and (d). The grain size of samples synthesized at this temperature is large (several micrometers). There are large regions in Fig. 8(d) in which there is no evidence for twins. The existence of these defects can also be observed through scanning electron microscopy.

The changes in the XRD patterns with synthesis temperature, obtained in this study, are in good general agreement with those obtained by simulations based on the presence of twins on the (001) plane of the rhombohedral B_4C structure. Figure 9 shows the simulated XRD patterns of B_4C with different stacking probabilities (α values). Several aspects of the patterns and their relation to the TEM observations require additional discussion. In Fig. 3 the pattern obtained at 2100°C shows no evidence of disorder (twins), despite the fact that the TEM micrograph (Fig. 8(d)) shows the presence of twins. This discrepancy relates to the density of twins, which as was indicated above, is low in samples synthesized at this high temperature (Fig. 8(c)). The explanation is consistent with our modeling studies. The simulation results, Fig. 9, show that little change is seen in the XRD patterns with low densities of twins, up to a probability (α) of about 0.10. Thus, despite their well-defined XRD pattern, samples synthesized at 2100°C (or synthesized at low temperature and subsequently annealed at this temperature) contain twins.

Another aspect related to the experimental XRD results concerns the relative intensities of the two main peaks (at 2θ values of about 38° and 35°) and their change with temperature. Careful examination of Fig. 6 reveals that the samples annealed at the lowest temperature (1300°C) show intensities of these two

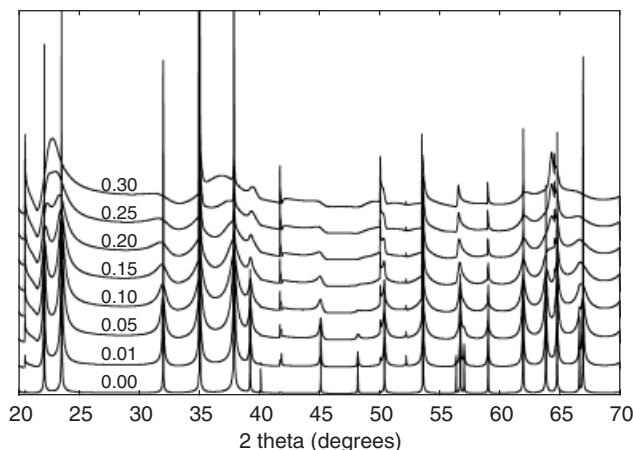


Fig. 9. Results of simulations showing the dependence of the X-ray diffraction pattern of boron carbide on the probability of twin occurrence, α .

peaks that are nearly equal and are inconsistent with the ratio obtained on samples annealed at 2100°C and that obtained in the modeling study (Fig. 9). At the highest temperature, the peak of the higher angle is significantly larger. The presence of twins can produce a significant change in peak width and a general decrease in intensity, but it is not expected to produce a change in the *relative* intensities of the peaks. However, the simulation study shows that the relative peak heights can be influenced by particle sizes considerations. Simulations were made with the same twin probability ($\alpha = 0.10$) but with different particle sizes (infinite and 10 nm) in the direction perpendicular to the plane of the twins. The results are presented in Fig. 10. A significant change in the relative intensities of the two main peaks is seen. For samples with large grains (here assumed infinitely large), the peak at 2θ of about 38° has a much higher intensity than the peak at about 35°. But when the grain size is assumed to be small (10 nm), the heights of these two peaks are comparable. As was indicated above, in a recent study on B_4C ⁷ it was shown that samples contained both large (a few micrometers) and small (nanometric) particles. Thus, a complete interpretation of the experimental XRD results must take into account the possible size inhomogeneity in samples. The change of the relative heights of the two peaks ($2\theta = 35^\circ$ and 38°) with temperature indicates the presence of small particles at low temperatures and the increase in their size with increasing temperature. These conclusions are consistent with TEM observations, as shown in Fig. 8.

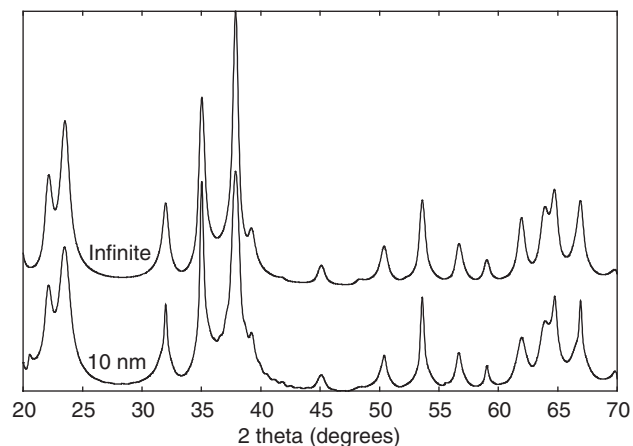


Fig. 10. Simulated X-ray diffraction patterns for boron carbide with two different crystallite sizes in the direction perpendicular to the twin plane, $\alpha = 0.20$.

V. Summary and Conclusion

The synthesis of dense (up to about 95% relative density) B_4C from the elements was made by field activation using the SPS method. Formation of B_4C commences at about 1000°C and is complete at 1200°C (with a hold time of 10 min). Significant densification occurs above 1600°C. XRD patterns from samples synthesized at temperatures ranging from 1300° to 2100°C showed evidence of extensive crystallographic disorder. Simulation study confirmed that this disorder is represented by twins on (001) plane. The degree of disorder decreased with an increase in temperature. TEM observations confirmed the presence of twins and their decrease with temperature. Peak relative intensity observations on experimental XRD patterns were consistent with simulation studies and TEM observations indicating the presence of small grains at lower temperatures and a larger one at the highest temperature.

References

- ¹B. A. Cook, J. L. Harringa, T. L. Lewis, and A. M. Russell, "A New Class of Ultra-Hard Materials Based on $AlMgB_{14}$," *Scripta Mater.*, **42**, 597–602 (2000).
- ²C. Emin and D. Wood, "Refractory Materials for High-Temperature Thermoelectric Energy Conversion," pp. 199–205 in *Materials Research Society Proceedings, Vol. 24, Defect Properties and Processing of High-Technology Nonmetallic Materials*, Edited by J. H. Crawford, Y. Chen, and W. A. Sibley. Materials Research Society, Boston, MA, 1984.
- ³F. Thevenot, "Boron Carbide—A Comprehensive Review," *J. Eur. Ceram. Soc.*, **6**, 205–25 (1990).
- ⁴C. Wood and D. Emin, "Conduction Mechanism in Boron Carbide," *Phys. Rev.*, **B29**, 4582–7 (1984).
- ⁵I. D. R. Mackinnon, T. L. Aselage, and S. B. Van Deusen, "High Resolution Imaging of Boron Carbide Nanostructures," *Am. Inst. Phys. Conf. Proc.*, [140] 114–20 (1986).
- ⁶B. Palosz, S. Gierlotka, S. Stelmakh, R. Pielaszek, P. Zinn, M. Winzenick, U. Bismayer, and H. Boysen, "High-Pressure High-Temperature *In Situ* Diffraction Studies of Nano Crystalline Ceramic Materials at HASYLAB," *J. Alloys Comp.*, **286**, 184–94 (1999).
- ⁷E. M. Heian, S. K. Khalsa, J. W. Lee, Z. A. Munir, T. Yamamoto, and M. Ohyanagi, "Synthesis of Dense, High Defect Concentration B_4C Through Mechanical Activation and Field-Assisted Combustion," *J. Am. Ceram. Soc.*, **87**[5], 779–83 (2004).
- ⁸M. Ohyanagi, T. Yamamoto, H. Kitaura, Y. Kodera, T. Ishii, and Z. A. Munir, "Consolidation of Nanostructured SiC with Disorder-Order Transformation," *Scripta Mater.*, **50**, 111–4 (2004).
- ⁹R. Orru, J. Woolman, G. Cao, and Z. A. Munir, "Synthesis of Dense Nanometric $MoSi_2$ Through Mechanical and Field Activation," *J. Mater. Res.*, **16**, 1439–48 (2001).
- ¹⁰A. Feng, T. Orling, and Z. A. Munir, "Field-Activated Pressure-Assisted Combustion Synthesis of Polycrystalline Ti_3SiC_2 ," *J. Mater. Res.*, **14**, 925–39 (1999).
- ¹¹V. Gauthier, F. Bernard, E. Gaffet, Z. A. Munir, and J. P. Larpin, "Synthesis of Nanocrystalline $NbAl_3$ by Mechanical and Field Activation," *Intermetallics*, **9**, 571–80 (2001).
- ¹²M. M. J. Treacy, J. M. Newsam, and M. W. Deem, "A General Recursion Method for Calculating Diffracted Intensities from Crystals Containing Planar Faults," *Proc. Roy. Soc. London*, **A433**, 499–520 (1991).
- ¹³M. L. Miller and I. D. R. Mackinnon, "A Comparison of Calculated and Experimental HRTEM Images for Twinned Boron Carbide," pp. 133–8 > in *Materials Research Society Proceedings, Vol. 97, Novel Refractory Semiconductors*, Edited by D. Emin, T. L. Aselage, and C. Wood. Materials Research Society, Pittsburgh, PA, 1987.
- ¹⁴S. L. Hoard and R. E. Hughes, "Elemental Boron and Compounds of High Boron Content: Structure, Properties, and Polymorphism," pp. 25–154 in *Chemistry of Boron and Its Compounds*, Edited by E. L. Muettterties. Wiley, New York, 1967.
- ¹⁵L. B. Pankartz, J. M. Stuve, and N. A. Gokcen, "Thermodynamic Data for Mineral Technology," US Bureau of Mines, Bulletin 677, 1984, U.S. Bureau of Mines, Washington, DC.
- ¹⁶A. Chakraborty, "Kinetics of the Reduction of Hematite to Magnetite Near Its Curie Temperature," *J. Magn. Magn. Mater.*, **204**, 57–60 (1999).
- ¹⁷H. Kobayashi, T. Terasaki, T. Mori, H. Yamamura, and T. Mitamura, "Preparation of $ZrSiO_4$ Powders by Sol–Gel Process. 3. Preparation Conditions of $ZrSiO_4$ Composition Precursor Gels from $Si(OC_2H_5)_4$ and $Zr(OiC_3H_7)_4$ Alkoxides," *J. Ceram. Soc. Jpn.*, **99**, 42–6 (1991).
- ¹⁸Y. Kanno, "Thermodynamic and Crystallographic Discussion of the Formation and Dissociation of Zircon," *J. Mater. Sci.*, **24**, 2415–20 (1989).
- ¹⁹G. I. Kalandadze, S. O. Shalamberridze, and A. B. Peikrishvili, "Sintering of Boron and Boron Carbide," *J. Solid State Chem.*, **154**, 194–8 (2000).
- ²⁰H. A. Sauer and J. R. Fisher, "Processing of Positive-Temperature-Coefficient Thermistors," *J. Am. Ceram. Soc.*, **43**, 297–301 (1960).
- ²¹T. Yamamoto, H. Kitaura, Y. Kodera, T. Ishii, M. Ohyanagi, and Z. A. Munir, "Consolidation of Nanostructured β -SiC by Spark Plasma Sintering," *J. Am. Ceram. Soc.*, **87**[8], 1436–41 (2004).
- ²²R. L. Prickett, R. L. Hough, and D. Earley, "The Unusual Line Structure in Powder Patterns of Pyrolytically Deposited Boron Compounds and Other Materials," *Adv. X-ray Anal.*, **10**, 221–33 (1967). □